Turk J Chem
33 (2009) , 249 – 256.

doi:10.3906/kim-0809-32

Water-Gas Shift Reaction over Bimetallic Pt-Ni/Al_2O_3 Catalysts

Burcu Selen ÇAĞLAYAN, Ahmet Erhan AKSOYLU*
Department of Chemical Engineering, Boğaziçi University, 34342 Bebek, İstanbul-TURKEY
e-mail: aksoylu@boun.edu.tr

Received 30.10.2008

The water-gas shift (WGS) activity of bimetallic Pt-Ni/Al_2O_3 catalysts was investigated in the temperature range 200-450 °C using an idealized feed composition consisting of 3% CO and 6%-10% H_2O. The effects of the Ni content, space velocity, and H_2O/CO ratio on the catalytic performance of the catalysts were studied. An increase in the Ni content and H_2O/CO ratio shifted the carbon monoxide conversion–temperature curve toward lower reaction temperatures. No detectable methane formation was observed in the catalytic reaction tests. The results indicate that Pt-Ni/Al_2O_3 catalysts are highly selective and active for water-gas shift reactions under idealized conditions.

Key Words: Water-gas shift, Pt-Ni, CO removal, high temperature shift (HTS).

Introduction

Proton exchange membrane fuel cells (PEMFCs) fueled by hydrogen are considered the most promising option for vehicular and small-scale residential heat and power applications.[1−3] With combined fuel processor-PEMFC systems, hydrogen, which has storage and distribution network problems, can be generated from hydrocarbons having well-established distribution networks. In a fuel processor, 3 catalytic reactions run in series aiming to produce CO-free hydrogen to be fed to a fuel cell: (i) reforming of hydrocarbons; (ii) water-gas shift (WGS) reaction for decreasing carbon monoxide concentration, while increasing hydrogen concentration; (iii) preferential carbon monoxide oxidation, which reduces carbon monoxide in the reformer product to levels that guarantee stable operation of PEMFCs without any loss of activity.[1] Since the water-gas shift reaction is

*Corresponding author

exothermic, reversible, equilibrium-limited, and the desired CO levels can be achieved at low temperatures, it is normally performed in 2 steps. In the first step a high-temperature shift (HTS) catalyst is used for reaction at 350-500 °C. The second step is performed on a low temperature shift (LTS) catalyst at 180-240 °C.[3] WGS catalysts for fuel cell applications should be active, thermally stable, resistant to poisoning, and highly selective for a wide range of H_2O/CO ratios. As conventional high temperature (Fe–Cr oxide) and low temperature (Cu–Zn–Al_2O_3) WGS catalysts cannot be used in fuel cell applications due to their disadvantages such as thermodynamic limitations at high temperatures, sensitivity to air, the need of long pre-conditioning, and slow kinetics at low temperatures, there has been interest in the development of non-pyrophoric noble metal based catalyst formulations supported on metal oxide carriers.[3]

Among the catalysts studied, Au/CeO_2[4–7] and Au supported on CeO_2, Al_2O_3, TiO_2, and ZrO_2 support combinations[8–10] have been reported to show high activities at low temperatures. However, the activity and stability of the gold supported catalysts depend highly on the catalyst preparation and pretreatment conditions.[11] Another ceria supported catalyst, Pt/CeO_2, has attracted interest and has been reported to be very active in the medium temperature range (300-400 °C).[3,12–14]

Platinum, as a noble metal, has attracted interest for use in mixed oxide supported water-gas shift catalysts: Pt/ZrO_2,[15,16] Pt/TiO_2,[17] Pt/CeO_2-ZrO_2,[18] Pt/Al_2O_3,[19,20] and Pt/CeO_2-Al_2O_3[21,22] are some examples of the catalysts tested for catalytic WGS activity at low and high temperature regions.

Al_2O_3 is a very high surface area support that has been reported to result in significant enhancement of activity, selectivity, and stability of dispersed noble metals for a number of catalytic reactions including WGS. Panagiotopoulou et al. have investigated the catalytic performance of Pt-Al_2O_3 and 0.5%Pt-MO_x-Al_2O_3 mixed oxide catalysts in the low and high temperature range of WGS reaction and reported that the Al_2O_3 supported catalysts become active at high temperatures (450 °C).[11] They also reported that Pt-MO_x-Al_2O_3 catalysts, where M=Co, Ni, Ti, Fe, and Cr, exceed Pt-Al_2O_3 catalysts in catalytic performance at lower temperatures.

In the present study, the effects of the Ni content, GHSV, and H_2O/CO ratio on the WGS activity of bimetallic Pt-Ni/Al_2O_3 catalysts, which were reported to have high activity for autothermal reforming of propane[23] and LPG[24,25] in our previous studies, were investigated. It should be noted that the Pt-Ni system showed secondary water gas shift activity under the autothermal reforming conditions used in those studies.[23–25]

Experimental

The thermally stable δ-Al_2O_3 support with BET surface area 81.6 $m^2 g^{-1}$ and particle size 250-354 μm was obtained by drying γ-Al_2O_3 (Alcoa) at 423 K for 2 h and then calcining it at 1173 K for 4 h. The monometallic 5-10-15 wt.% Ni/δ-Al_2O_3 support was prepared by the incipient-to-wetness impregnation technique using aqueous precursor solution of $Ni(NO_3)_2 \cdot 6H_2O$ (Merck) having concentrations according to the targeted Ni loadings. For each sample, the resulting slurry that was formed after ultrasonic mixing of the precursor solution and the support under vacuum for 1.5 h was dried overnight at 393 K and then calcined at 873 K for 4 h. Pt was then added by the sequential impregnation technique of an aqueous solution of Pt, $Pt(NH_3)_4(NO_3)_2$ (Aldrich), over initially prepared and calcined NiO/δ-Al_2O_3. The platinum metal loading was kept fixed as

0.2 wt.% for all samples. Upon Pt impregnation, the final slurry was dried at 393 K and re-calcined at 773 K for 4 h.

The structural analyses and the phase identification of the Pt–Ni catalyst were carried out at Boğaziçi University Advanced Technologies R&D Center. The microstructure of the powder was examined using a Philips XL30 ESEM-FEG system with a maximum resolution of 2 nm. The crystalline phases of the Pt–Ni catalyst sample were identified using Rigaku D/MAX-Ultima+/PC X-Ray diffraction equipment having an X-ray generator with Cu target and scan speed of 2°/min. Quantitative elemental analyses were performed using energy dispersive spectroscopy (EDS) with a minimum detection limit of 50 ppm.

Reaction tests were conducted in a down-flow, 55 cm long 1/4 in. OD, stainless steel tubular microreactor. The catalyst bed was fixed in the middle of the reactor by glasswool. The bed height was less than 0.3 cm; thus, neither pressure gradient nor channeling was encountered in the reactor. The temperature of the catalyst bed was controlled with ± 0.1 K precision via a programmable temperature controller (Eurotherm 3216P). The flow rates of high purity gases supplied from high-pressure gas cylinders (hydrogen, carbon monoxide, nitrogen) were controlled by Brooks mass flow controllers. The water flow rate was controlled by an Agilent 1100 HPLC pump; water fed to the system was evaporated before it was introduced into the feed gas mixture.

In the analysis block of the system, 2 salt–ice traps were used to remove water vapor from the product stream. Transfer lines of the reactor and analysis parts of the system were kept at 398 K to prevent possible condensation. Two Agilent Technologies 6850 gas chromatographs equipped with a Porapak Q and Molecular Sieve 5A columns were used for analyzing CO_2 and fixed gasses, respectively. Blank tests confirmed that the stainless steel reactor and glasswool were inert under the reaction conditions.

The experiments were carried out in the temperature range 473-723 K. The reaction was studied at 50 K intervals starting from 473 K within the temperature range. Prior to reaction tests, the catalyst was reduced in 50 mL/min of pure hydrogen flow at 773 K for 2 h. The experiments were designed to investigate the effects of reaction parameters such as temperature, Ni content, steam/carbon monoxide ratio (H_2O/CO), and space velocity on the activity and selectivity of the catalyst in WGS. The reaction conditions are given in the Table. Experiments were duplicated and, in some cases, triplicated.

Table. The WGS reaction conditions studied over the bimetallic Pt-Ni/Al_2O_3 system.

#	Ni %	GHSV ($mLg^{-1}h^{-1}$)	H_2O/CO	CO (mL/min)	Total (mL/min)
1	5	120,000	10/3	4.5	150
2	10	120,000	10/3	4.5	150
3	15	120,000	10/3	4.5	150
4	5	120,000	2	4.5	150
5	10	120,000	2	4.5	150
6	15	120,000	2	4.5	150
7	5	60,000	10/3	4.5	150
8	15	60,000	10/3	4.5	150
9	5	180,000	10/3	4.5	150
10	15	180,000	10/3	4.5	150

Results and Discussion

The detailed catalyst characterization of Pt-Ni/Al_2O_3 samples has been reported previously[23,24] showing the changes on the catalyst surface and active metallic sites due to reduction. In this study, the crystalline phases were identified and no alloy formation was observed by either XRD or EDS analyses. SEM and EDS studies show that Ni particles cover almost the whole Al_2O_3 surface; the detailed mapping at high magnification showed that Pt-rich Pt and Ni islands are formed on the catalyst surface where Pt centers are located very close to Ni sites. In the X-ray analytical mapping images (Figure 1) these Pt and Ni sites are clearly distinguished. As the nickel content is increased from 5% to 10%, distinct and bigger Ni islands are formed, which makes it possible for more platinum atoms to come into direct contact with Ni atoms. Therefore, it can easily be assumed that the Pt-Ni interaction is more effective for the samples that have higher Ni contents.

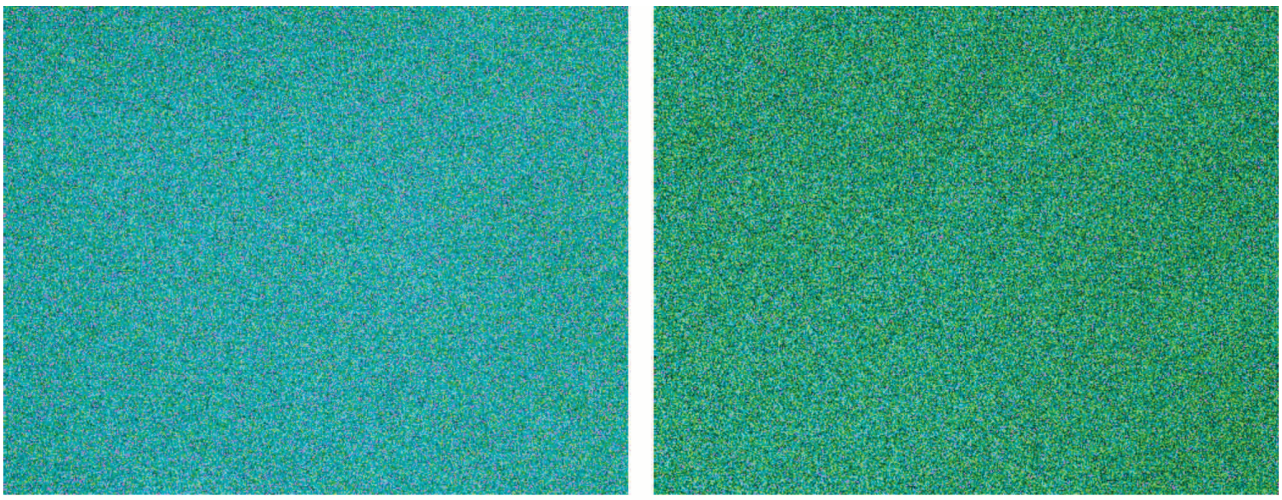

(a) (b)

Figure 1. X-ray analytical mapping image of 0.2%Pt-5%Ni/Al_2O_3 (a) and 0.2%Pt-15%Ni/Al_2O_3 (b). Al_2O_3: Blue; Ni: Green; Pt: Purple. (Magn: 100,000×).

The results presented were obtained using an idealized feed composition consisting of 3% CO, 6%-10% H_2O, and 87%-91% inert, resembling the feed composition generally used for LTS reaction; in the literature, a typical reformate sent to the WGS reactors of a fuel processor contains 8%-10% and 3%-5% CO for HTS and LTS reactors,[3] respectively, and H_2O/CO ratio in those feeds is 1-3.5 and >3.5 for LTS and HTS, respectively. The temperature level used in the current work corresponds to the HTS-LTS transition range. The results of catalytic performance tests obtained over bimetallic catalysts with different nickel amounts are shown in Figure 2. For each test, the H_2O/CO ratio and GHSV were 10/3 and 120,000 mL/g.h, respectively. With the increase in Ni loading, equilibrium conversions can be reached at lower temperatures. In the literature, there are several factors proposed to be responsible for the enhancement in the catalytic activity of the metal oxide(s) promoted noble metal catalysts supported on high surface area oxide supports**.** These factors are as follows: increased reducibility of the support,[11,26] stabilization of the noble metal crystallites against sintering,[11,27] and formation of new active sites.[11,26,27] Therefore, the increase in the amount of nickel added may have strengthened one or more of these effects in the current study. Furthermore, Pt crystallites, which are in direct contact with

the reducible NiO_x species confirmed by our catalyst characterization studies, are also responsible for the enhancement of activity; as the Ni loading was increased, the Pt-Ni interaction was enhanced.

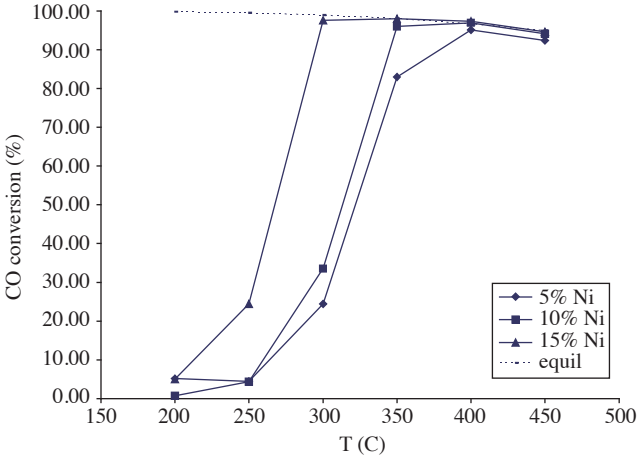

Figure 2. Effect of Ni loading of Pt-Ni catalysts on WGS activity profile given as a function of temperature. Equilibrium conversion is also indicated. (3% CO; 10% H_2O; 87% N_2).

The effect of H_2O/CO ratio on WGS activity was investigated using 2 different ratios: 10/3 and 2 (Figure 3). The results showed that H_2O/CO has a similar effect on carbon monoxide conversion as Ni loading: with the increase in H_2O/CO ratio, CO conversion increases and equilibrium conversions can be reached at lower temperatures. The results are very reasonable since the equilibrium conversion of carbon monoxide for an H_2O/CO ratio of 10/3 is higher than that of an H_2O/CO ratio of 2 for the temperature range studied, as shown in Figure 3. It should be noted that the equilibrium conversion levels, which were calculated by HSC Chemistry software, are given in Figures 2 and 3 for the reaction conditions used.

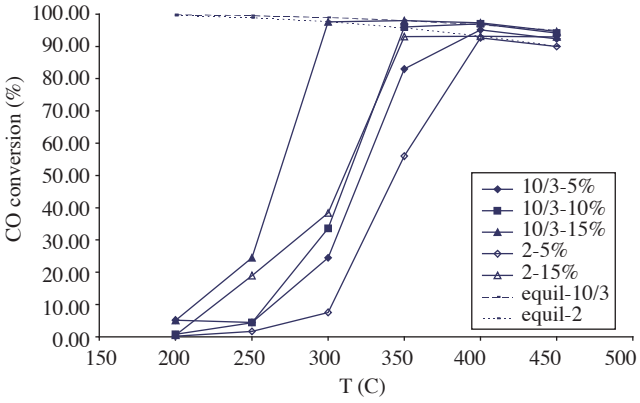

Figure 3. Effect of H_2O/CO ratio on WGS activity profile given as a function of temperature. Equilibrium conversions are also indicated.

To investigate the effect of GHSV on the catalytic activity, the flow rate of the reaction mixture was kept unchanged, whereas the amount of catalyst was varied. No significant trend in the CO conversion was

observed with increasing GHSV for the whole temperature range (Figure 4), although an enhancement in WGS activity would be expected with a decrease in space velocity. According to our results so far, it is very obvious that there should be an optimum space velocity value for the water-gas shift reaction conditions that are studied (Figure 5); the maximum values observed in CO conversion level-GHSV profiles for tests conducted over different catalysts at different temperature levels clearly indicate that the conversion level is imposed by a balance between rate of reaction and space velocity, which should be studied further in order to find optimum "reaction condition-catalyst composition" combination(s).

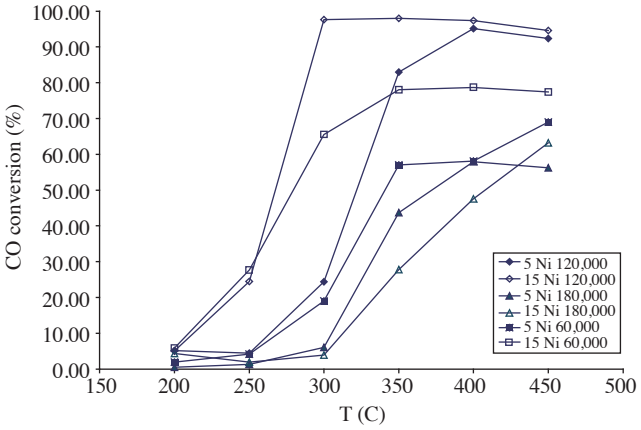

Figure 4. Effect of space velocity on WGS activity profile given as a function of temperature. (3% CO; 10% H_2O; 87% N_2).

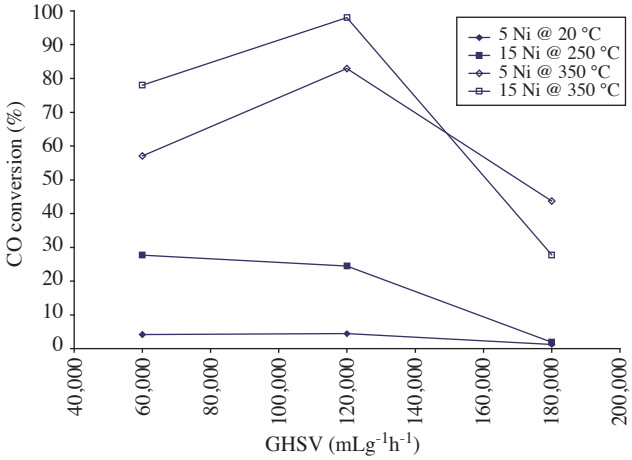

Figure 5. CO conversion as a function of GHSV (3% CO; 10% H_2O; 87% N_2).

Selectivity is one of the most important qualities of a water-gas shift reaction catalyst: side reactions, especially methanation, that would consume hydrogen should be avoided for a range of H_2O/CO ratios and space velocities.[3] No detectable methane formation was observed in the catalytic reaction tests conducted using different idealized feed compositions.

Acknowledgements

This work was supported by TÜBİTAK through project 105M282 and DPT (State Planning Organization of Turkey) through project DPT07K120630 and DPT03K120250. A.E. Aksoylu acknowledges the support provided by the TÜBA-GEBIP program.

References

1. Trimm, D. L.; Önsan, Z. İ. *Catal. Rev.* **2001**, *43*, 31-84.
2. Ahmet, S.; Krumpelt, M. *Int. J. Hydrogen Energy* **2001**, *26*, 291-301.
3. Ghenciu A.F. *Curr. Opin. Solid State Mater. Sci.* **2002**, *6*, 389-399.
4. Denkwitz, Y.; Karpenko, A.; Plzak, V.; Leppelt, R.; Schumacher, B.; Behm, R. J. *J. Catalysis* **2007**, *246*, 74-90.
5. Fu, Q.; Weber, A.; Flytzani-Stephanopoulos, M. *Catalysis Letters* **2001**, *77*, 87-95.
6. Fu, Q.; Kudriavtseva, S.; Saltsburg, H.; Flytzani-Stephanopoulos, M. *Chem. Eng. J.* **2003**, *93*, 41-53.
7. Deng, W.; De Jesus, J.; Saltsburg, H.; Flytzani-Stephanopoulos, M. *App. Cat. A: Gen.* **2005**, *291*, 126-135.
8. Idakiev, V.; Tabakova, T.; Tenchev, K; Yuan, Z. Y.; Ren, T. Z.; Su, B. L. *Catalysis Today* **2007**, *128*, 223-229.
9. Sandoval, A.; Gomez-Cortez, A.; Zanella, R.; Diaz, G.; Saniger, J. M. *J. Mol. Catalysis A: Chem* **2007**, *278*, 200-208.
10. Li, J.; Chen, J.; Song, W.; Liu, J; Shen, W. *App. Cat. A: Gen.* **2008**, *334*, 321-329.
11. Panagiotopoulou, P.; Kondarides, D. I. *Catalysis Today* **2007**, *127*, 319-329.
12. Meunier, F. C.; Goguet, A.; Hardacre, C.; Burch, R.; Thompsett, D. *J. Catalysis* **2007**, *252*, 18-22.
13. Meunier, F. C.; Tibiletti, D.; Goguet, A.; Shekhtman, S.; Hardacre, C.; Burch, R. *Catalysis Today* **2007**, *126*, 143-147.
14. Duarte de Farias, A. M.; Barandas, A. P. M. G.; Perez, R. F.; Fraga, M. A. *J. Power Sources* **2007**, *165*, 854-860.
15. Lee, H. C.; Lee, D.; Lim, O. Y.; Kim, S.; Kim, Y. T.; Ko, E. Y.; Park, E. D. *Stud. Surf. Sci. Catalysis,* **2007**, *167*, 201-206.
16. Pigos, J. M.; Brooks, C. J.; Jacobs, G.; Davis, B. H. *App. Cat. A: Gen.* **2007**, *328*, 14-26.
17. Azzam, K. G.; Babich, I. V.; Seshan, K.; Lefferts, L. *App. Cat. A: Gen.* **2008**, *338*, 66-71.
18. Querino, P. S.; Bispo, J. R. C.; Rangel, M. C. *Catalysis Today* **2005**, *107-108*, 920-925.
19. Olympiou, G. G.; Kalamaras, C. M.; Zeinalipour-Yazdi, C. D.; Efstathiou, A. M. *Catalysis Today* **2007**, *127*, 304-318.
20. Phatak, A. A.; Koryabkina, N.; Rai, S.; Ratts, J. L.; Ruettinger, W.; Blau, G. E.; Delgass, W. N.; Ribeiro, F. H. *Catalysis Today* **2007**, *123*, 224-234.
21. Haryanto, A.; Fernando, S.; Adhikari, S. *Catalysis Today* **2007**, *129*, 269-274.
22. Germani, G.; Alphonse, P.; Courty, M.; Schuurman, Y.; Mirodatos, C. *Catalysis Today* **2005**, *110*, 144-120.
23. Çağlayan, B. S.; Avcı, A. K.; Önsan, Z. İ.; Aksoylu, A. E. *App. Cat. A: Gen.* **2005**, *280*, 181-188.

24. Çağlayan, B. S.; Önsan, Z. İ.; Aksoylu, A. E. *Catalysis Letters* **2005**, *102*, 63-67.
25. Gökaliler, F.; Çağlayan, B. S.; Önsan, Z. İ.; Aksoylu, A. E. *Int. J. Hyd. Energy* **2008**, *33*, 1383-1391.
26. Damyanova, S.; Bueno, J. M. C. *App. Cat. A: Gen.* **2003**, *253*, 135-150.
27. Grisel, R. J. H.; Nieuwenhuys, B. E. *Catalysis Today* **2001**, *64*, 69-81.